

PROCEEDINGS IRF2016

5th International Conference INTEGRITY-RELIABILITY-FAILURE

Porto/Portugal, 24-28 July 2016

Editors

J.F. Silva Gomes (*FEUP, U. Porto*)
Shaker A. Meguid (*MADL, U. Toronto*)

ISBN: 978-989-98832-5-3

INEGI/FEUP
(2016)

ENTER

J.F. Silva Gomes
Shaker A. Meguid
Editors

IRF2016

**Proceedings of the 5th International
Conference on
Integrity - Reliability - Failure**

Porto/Portugal, 24-28 July 2016

**FEUP-INEGI
(2016)**

IRF2016

**Proceedings of the 5th
International Conference on
INTEGRITY-RELIABILITY-FAILURE**

IRF2016

Proceedings of the 5th International Conference on INTEGRITY-RELIABILITY-FAILURE

Editors

J.F. Silva Gomes and Shaker A. Meguid

**FEUP-INEGI
(2016)**

Published by

INEGI-Instituto de Ciência e Inovação em Engenharia Mecânica e Gestão Industrial
Rua Dr Roberto Frias, 4200-465 Porto - Portugal
Tel: +351 22 9578710; Email: inegi@inegi.up.pt
<http://www.inegi.up.pt/>

July, 2016

ISBN: 978-989-98832-5-3

All rights reserved. No part of this publication may be reproduced, stored in a retrieval system, or transmitted in any form or by any means, electronic, mechanical, optical, recording, or otherwise, without the prior written permission of the Editors

TABLE OF CONTENTS

Preface	xix
International Scientific Committee	xx
Organizing Committee and Secretariat	xxi
Acknowledgments	xxii
List of Tracks and Symposia	xxiii
KEYNOTE PAPERS	1
6101 COMPUTATIONAL CONTACT MECHANICS USING VARIATIONAL INEQUALITIES: THEORY AND APPLICATIONS. Shaker A. Meguid	3
6102 CRASHWORTHINESS OF HYBRID METAL / FIBER-REINFORCED PLASTIC STRUCTURES. Thomas Tröster, Corin Reuter, Zheng Wang	5
6103 MDO APPROACH TO OPTIMAL VARIABLE STIFFNESS STRUCTURE DESIGN. Michel J.L. van Tooren	7
TRACKS / MAIN TOPICS	9
TOPIC-A: COMPUTATIONAL MECHANICS	11
6194 STOCHASTIC EFFECTS OF CRACKED BEAMS SUBJECTED TO RANDOM MOVING LOADS. H. S. Zibdeh, Y. Qaissi	13
6203 NUMERICAL EVALUATION OF THE MIXED-MODE FRACTURE OF COMPOSITE BONDED JOINTS. Manuel A.S. Santos, Raul D.S.G. Campilho	15
6238 TRANSIENT ELASTICITY MODELING OF WAVE-SHAPE FORMATION UNDER EXPLOSION WELDING. Ireneusz Szachogluchowicz, Lucjan Sniezek, Volodymyr Hutsaylyuk, Heorhiy Sulym, Iaroslav Pasternak, Ihor Turchyn	17
6251 CONFIDENCE BOUNDS ON PROBABILITY OF FAILURE USING MHDMMR. A. S. Balu, B. N. Rao	27
6257 SIMULATION OF THE INFLUENCE OF STEEL FIBERS ON THE SHEAR BEHAVIOR OF REINFORCED CONCRETE BEAMS. Mohand Said Kachi, Zarga Djelloul, Barboura Salma, Bouafia Youcef	35
6264 MODAL ANALYSIS OF A SOLID RUNNER FOR SMALL WIND TURBINES. Nicolae Constantin, Ștefan Sorohan, Constantin Valentin Epuran	41
6357 AXIAL BUCKLING RESISTANCE OF PARTIALLY ENCASED COLUMNS. Abdelkadir Fellouh, Nourredine Benlakehal, Paulo A. G. Piloto, A. B. Ramos-Gavilán, Luís M. R. Mesquita	47
6371 SHORTCUT ESTIMATION OF CONFIDENCE IN THE OUTCOME OF THE VULNERABILITY ASSESSMENT OF A STRUCTURAL SYSTEM WITH CAPACITY EXPRESSED BY A FUNCTION G. Marco Vailati, Giorgio Monti, Giovanna Valeri	57
6377 NUMERICAL EVALUATION OF THE BEHAVIOR OF TUBULAR COLUMNS IN THE CONNECTIONS TO I BEAMS WITH WELDED REVERSE CHANNEL. Luís Magalhães, Carlos Rebelo, Sandra Jordão	59

International Scientific Committee

Aben, H. (Estonia)	Degrieck, J. (Belgium)	Mal, A. (USA)	Seabra, Jorge (Portugal)
Adali, S. (S. Africa)	Dietrich, L. (Poland)	Marques, A.T. (Portugal)	Semenski, D. (Croatia)
Afonso, C.F. (Portugal)	Eberhardsteiner, J. (Austria)	Masato, Y. (Japan)	Silva Gomes, J.F. (Portugal)
Alexopoulos, N. (Greece)	Fernandes, A.A. (Portugal)	Meda, A. (Italy)	Sjödahl, M. (Sweden)
António, C.C. (Portugal)	Ferreira, D. (Portugal)	Meguid, S.A. (Canada)	Sousa, L.C. (Portugal)
Banks-Sills, L. (Israel)	Ferreira, J.G. (Portugal)	Mileiko, S.T. (Russia)	Takagi, T. (Japan)
Baptista, J.S. (Portugal)	Fiúza, A. (Portugal)	Miller, R.E. (Canada)	Tamalsky, E. (Brazil)
Barros, R.C. (Portugal)	Fonseca E. (Portugal)	Mines, R. (UK)	Tamuzs, V. (Latvia)
Bathe, K.J. (USA)	Gdoutos, E. (Greece)	Moreira, P. (Portugal)	Tavares, J.M. (Portugal)
Botsis, J. (Switzerland)	Hejum, Du (Singapore)	Morimoto, Y. (Japan)	Tavares, P. (Portugal)
Braz-César, M. (Portugal)	Igartua, A. (Spain)	Moura, M.F. (Portugal)	Tooren, M.J. (Netherlands)
Caetano, E. (Portugal)	Ignaszak, Z. (Poland)	Muc, Aleksander (Poland)	Truman, C.E. (UK)
Camanho, P. (Portugal)	Iliescu, N. (Romania)	Noroozinejad, E. (Iran)	Turmanidze, R. (Georgia)
Campos, J.R. (Portugal)	Jones, N. (UK)	Pappalettere, C. (Italy)	Umehara, N. (Japan)
Campos, Vicente (Portugal)	Jorge, R.N. (Portugal)	Pieczyska, E. (Poland)	VanHemelrijck, D. (Belgium)
Castro, C.F. (Portugal)	Kahlen, F-J. (S. Africa)	Piloto, P. (Portugal)	Varum, H. (Portugal)
Castro, P.T. (Portugal)	Klein, W. (Germany)	Pindera, M.J. (USA)	Vaz, Mário P. (Portugal)
Chen, T. (Taiwan)	Kourkoulis, S. (Greece)	Quelhas, O. (Brazil)	Wang, Wei-Chung (Taiwan)
Chenot, J-L (France)	Laermann, K. (Germany)	Ramesh, K. (India)	Weng, G. (USA)
Cirne, J. (Portugal)	Langseth, M. (Norway)	Reddy, J.N. (USA)	Yang, Fan (China)
Correia, A. (Portugal)	Lima, G. (Brazil)	Robinson, J. (Ireland)	Yoneyama, Satoru (Japan)
Croccolo, D. (Italy)	Lino, J. (Portugal)	Ruiz, G. (Spain)	Yong, N.T. (Singapore)
Cunha, A. (Portugal)	Lopes, H. (Portugal)	Ruzicka, M. (Czech R.)	Yoon, Y.C. (Singapore)
Datta, S. (USA)	Lu, Jian (Hong Kong)	Sainov, V. (Bulgaria)	Zhang, Z. (China)

Institutional Sponsors

FEUP

*University of Porto
Portugal*

MADL

*University of Toronto
Canada*

Co-Chairs

J.F. Silva Gomes (*U. Porto*)

Shaker A. Meguid (*U. Toronto*)

Organizing Committee

Carlos C. António, Catarina F. Castro, Clito F. Afonso, José M. Cirne
Mário A.P. Vaz, Paulo G. Piloto, Pedro M.G.P. Moreira

Conference Secretariat

Nuno Pinto, Lurdes Catalino

With the support of

ABREU-PCO, Professional Congress Organizer (<http://pco.abreu.pt>)
Mercatura Conference System (<http://www.mercatura.pt>)

PAPER REF: 6357

AXIAL BUCKLING RESISTANCE OF PARTIALLY ENCASED COLUMNS

Abdelkadir Fellouh¹, Nourredine Benlakehal¹, Paulo A. G. Piloto^{2(*)}, A. B. Ramos-Gavilán³,
Luís M. R. Mesquita⁴

¹University Hassiba Benbouali (UHBC), Chlef, Algeria

²LAETA-INEGI, Department of Applied Mechanics, Polytechnic Institute of Bragança (IPB), Portugal

³Department of Mechanical Engineering, University of Salamanca (USAL), Spain

⁴ISISE, Department of Applied Mechanics, Polytechnic Institute of Bragança (IPB), Portugal

(*)Email: ppiloto@ipb.pt

ABSTRACT

Partially Encased Columns (PEC) present good axial buckling resistance under fire, mainly due to the presence of concrete between flanges. The presence of concrete increases the mass and thermal inertia of the member and changes the variation of the temperature field within the cross section, in both the steel and concrete. The elastic buckling load of PEC under fire conditions may be calculated by the balanced summation method and by the finite element method. This work compares the results from both solution methods and provides the validation of the three dimensional model for different fire ratings of 30 and 60 minutes.

Keywords: Partially encased columns, buckling load, fire resistance.

INTRODUCTION

Partially encased columns are usually made of hot rolled steel profiles, reinforced with concrete between the flanges. The composite section is responsible for increasing axial, torsional and bending stiffness when compared to the bare steel solution. The reinforced concrete is also responsible for increasing the fire resistance. In a composite column, both the steel and concrete are expected to resist the external loading by interacting together by bond and friction. Supplementary reinforcement in the concrete encasement prevents excessive spalling of concrete both under normal load and fire conditions. Due to the thermal and mechanical properties of concrete, composite columns always presents higher fire resistance than the corresponding steel bare columns.

Two methods are used to determine the elastic buckling resistance: the simple calculation method and the advanced calculation method. For convenience, the elastic buckling resistance is presented in non-dimensional format, using the no dimensional slenderness at elevated temperature and ratio between the elastic buckling resistance and the plastic axial resistance, both for 30 and 60 minutes of ISO834 fire.

PARTIALLY ENCASED COLUMNS

Twenty-four different cross sections were selected to study the effect of fire: ten steel IPE profiles ranging from 200 to 500 and fourteen steel HEB ranging from 160 to 500. The columns were tested under ISO834 fire, using one buckling length, corresponding to pinned

end boundary conditions, using 3m column height. S275 and B500 grades were selected to steel while C20/25 grade was considered to concrete.

The cross sections were defined accordingly to the tabular design method for partially encased columns under fire (CEN, 2005). This leads to minimum dimensions and minimum distances between components. The design of these sections depends on the load level, and on the ratio between the thickness of the web and the thickness of the flange, see Fig. 1. This tabular method applies to structural steel grades S235, S275 and S355 and to a minimum value of reinforcement, between 1 and 6%. Table 1 presents the main dimensions, in particular the number of rebars, the diameter of each rebar, the cover dimensions in both principal directions

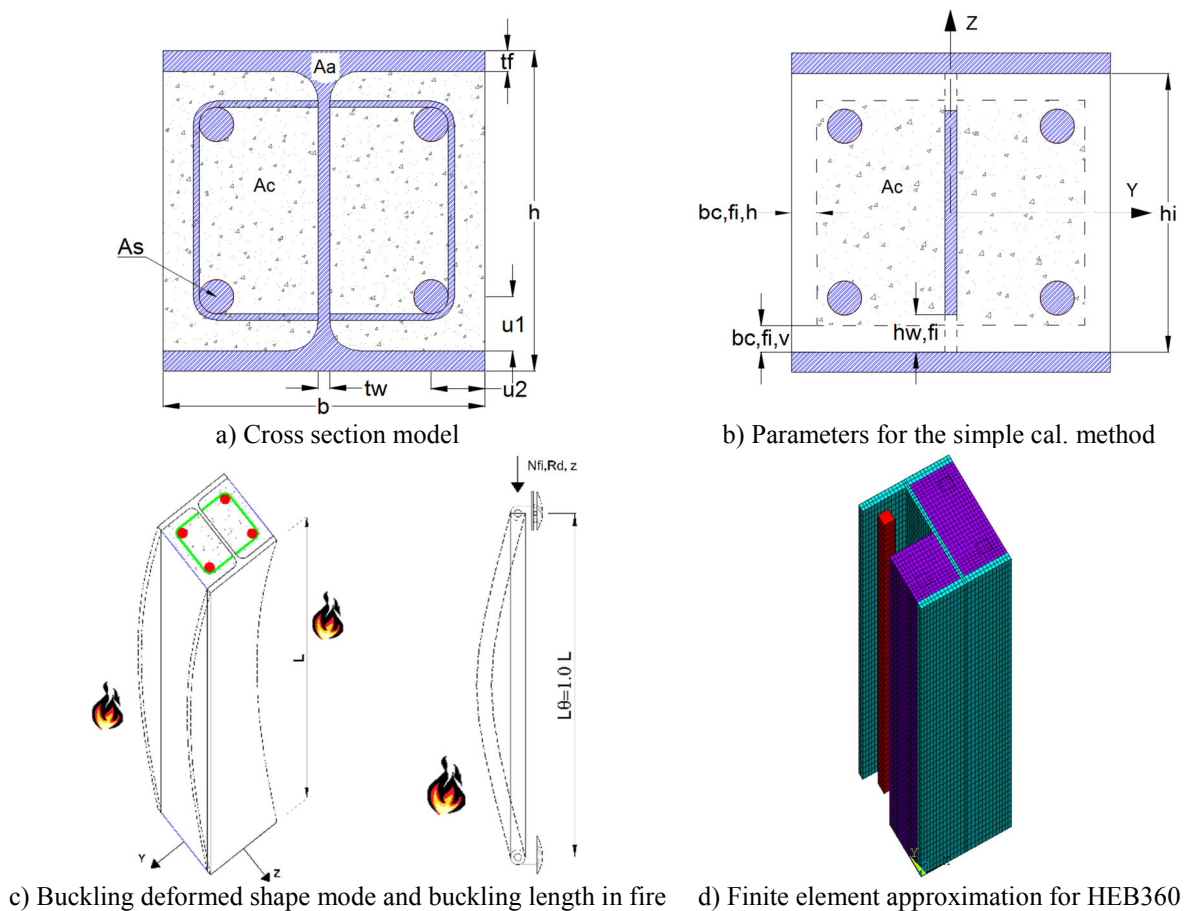


Fig. 1 - Partially encased column under fire.

The fire resistance of partially encased columns may be calculated by the balanced summation method, which is based on the contribution of four components and depends on the temperature effect in each component. According to Eurocode 4, Part 1.2 (CEN, 2005), the fire resistance can be evaluated by this method, see annex G, considering the flanges of steel profile, the web of steel profile, the concrete and the reinforcement submitted to standard fire and for different fire resistance classes (R30 and R60). This method presents a few empirical coefficients that were rectified, but similar formulas are presented. These new results are much safer than the ones presented in Eurocode 4, Part 1.2 (CEN, 2005).

This paper aims to compare the results of the elastic buckling load, when calculated by the new proposal to the balanced summation method (Paulo Piloto et al, 2015) and the results of a fully three-dimensional model, herein presented.

Table 1 - Section properties for partially encased columns.

Profile	Rebars	h_i mm	Φ mm	A_s mm ²	A_c mm ²	u_1 mm	u_2 mm	u mm	$A_s / A_s + A_c$	t_w / t_f	A_m / V m ⁻¹
HEB160	4	134.0	12	452	19916	40	40	40	2,22	0,62	25.00
HEB180	4	152.0	12	452	25616	40	40	40	1,74	0,61	22.22
HEB200	4	170.0	20	1257	31213	50	50	50	3,87	0,60	20.00
HEB220	4	188.0	25	1963	37611	50	50	50	4,96	0,59	18.18
HEB240	4	206.0	25	1963	45417	50	50	50	4,14	0,59	16.67
HEB260	4	225.0	32	3217	53033	50	50	50	5,72	0,57	15.38
HEB280	4	244.0	32	3217	62541	50	50	50	4,89	0,58	14.29
HEB300	4	262.0	32	3217	72501	50	50	50	4,25	0,58	13.33
HEB320	4	279.0	32	3217	77275	50	50	50	4,00	0,56	12.92
HEB340	4	297.0	40	5027	80509	50	50	50	5,88	0,56	12.55
HEB360	4	315.0	40	5027	85536	50	50	50	5,55	0,56	12.22
HEB400	4	352.0	40	5027	95821	70	50	59	4,98	0,56	11.67
HEB450	4	398.0	40	5027	108801	70	50	59	4,42	0,54	11.11
HEB500	4	444.0	40	5027	121735	70	50	59	3,97	0,52	10.67
IPE200	4	183.0	12	452	16823	50	40	45	2,62	0,66	30.00
IPE220	4	201.6	20	1257	19730	50	40	45	5,99	0,64	27.27
IPE240	4	220.4	20	1257	23825	50	40	45	5,01	0,63	25.00
IPE270	4	249.6	25	1963	30085	50	40	45	6,13	0,65	22.22
IPE300	4	278.6	25	1963	37848	50	40	45	4,93	0,66	20.00
IPE330	4	307.0	25	1963	44854	50	40	45	4,19	0,65	18.56
IPE360	4	334.6	32	3217	50988	50	40	45	5,93	0,63	17.32
IPE400	4	373.0	32	3217	60715	70	40	53	5,03	0,64	16.11
IPE450	4	420.8	32	3217	72779	70	40	53	4,23	0,64	14.97
IPE500	4	468.0	40	5027	83800	70	50	59	5,66	0,64	14.00

BALANCED SUMMATION METHOD

This method requires analytical formulas to take into consideration the effect of the fire (ISO, 1999) in four components, assuming the same methodology of EN1994-1-2 annex G (CEN, 2005). For the calculation of the critical load, the effective flexural stiffness needs to be determined. This quantity depends on the temperature effect on the elastic modulus and on the second order moment of area of four components, according to Eq. 1.

$$(EI)_{fi,eff,z} = \varphi_{f,\theta}(EI)_{fi,f,z} + \varphi_{w,\theta}(EI)_{fi,w,z} + \varphi_{c,\theta}(EI)_{fi,c,z} + \varphi_{s,\theta}(EI)_{fi,s,z} \quad (1)$$

In this equation $(EI)_{fi,eff,z}$ represents the effective flexural stiffness of the composite section in fire, $(EI)_{fi,f,z}$ represents effective flexural stiffness of the flange, $(EI)_{fi,w,z}$ represents effective flexural stiffness of the web, $(EI)_{fi,c,z}$ represents the effective flexural stiffness of the concrete and $(EI)_{fi,s,z}$ represents the effective flexural stiffness of reinforcement. The contribution of each part is going to be weighted according to φ factors, see Table 2.

Table 2 - Reduction coefficients for bending stiffness around the weak axis.

Standard fire resistance	$\varphi_{f,\theta}$	$\varphi_{w,\theta}$	$\varphi_{c,\theta}$	$\varphi_{s,\theta}$
R30	1,0	1,0	0,8	1,0
R60	0,9	1,0	0,8	0,9
R90	0,8	1,0	0,8	0,8
R120	1,0	1,0	0,8	1,0

The elastic buckling load $N_{fi,cr,z}$ requires the calculation of the axial plastic resistance under fire $N_{fi,pl,Rd}$. The non-dimensional slenderness ratio $\bar{\lambda}_\theta$ is also presented in Eqs. 2-4, when the safety partial factors are assumed equal to 1.0. L_θ represents the buckling length of the column under fire conditions.

$$N_{fi,pl,Rd} = N_{fi,pl,Rd,f} + N_{fi,pl,Rd,w} + N_{fi,pl,Rd,c} + N_{fi,pl,Rd,s} \quad (2)$$

$$\bar{\lambda}_{\theta} = \sqrt{N_{fi,pl,Rd} / N_{fi,cr,z}} \quad (3)$$

$$N_{fi,cr,z} = \pi^2 / L_{\theta}^2 \times (EI)_{fi,eff,z} \quad (4)$$

The effect of fire in the flange component requires a bilinear approximation for the calculation of the average temperature in flange, using a new empirical coefficient k_t and a new reference value $\theta_{0,t}$, see Eq. 5 and Table 3. The temperature is affecting the elastic modulus of the material without any other reduction that could affect the second order moment of area.

$$\theta_{f,t} = \theta_{0,t} + k_t(A_m/V) \quad (5)$$

Table 3 - Parameters to determine flange temperature (Section HEB and IPE).

Sections	10 < Am/V < 14		14 ≤ Am/V < 25		10 < Am/V < 19		19 ≤ Am/V < 30	
Standard	HEB		HEB		IPE		IPE	
Fire	$\theta_{0,t}$ [°C]	k_t [m°/C]	$\theta_{0,t}$ [°C]	k_t [m°/C]	$\theta_{0,t}$ [°C]	k_t [m°/C]	$\theta_{0,t}$ [°C]	k_t [m°/C]
R30	387	19,55	588	4,69	582	6,45	656	2,45
R60	665	14,93	819	3,54	824	3,75	862	1,72
R90	887	5,67	936	2,04	935	2,20	956	1,09
R120	961	4,29	998	1,62	997	1,68	1010	0,96

The effect of fire on the web of the steel section was determined by the 400 °C isothermal criterion (Cajot et al, 2012) (R. Zaharia, 2011) (R. Zaharia, 2012). This procedure defines the affected zone of the web and predicts the web height reduction $h_{w,fi}$, see Fig. 1. This new formulae (Paulo Piloto et al, 2015) presents a strong dependence on the section factor, regardless of the fire resistance class (t in minutes), unlike the simplified method of EN1994-1-2 (CEN, 2005). The results of EN1994-1-2 are unsafe for all fire resistance classes and for all section factors. The new proposal presents a parametric expression that depends on section factor and standard fire resistance class, Eqs. 6-7. Both equations have the application limits defined in Table 4. This calculation is affecting the second order moment of area of the web, without considering any temperature effect on the reduction of the elastic modulus.

$$2h_{w,fi} / h_i \times 100 = 0.0035 \times t^2 \times (A_m/V) - 0.03 \times t^{2.02} + (A_m/V) / 2 \quad , (HEB) \quad (6)$$

$$2h_{w,fi} / h_i \times 100 = 0.002 \times t^2 \times (A_m/V) - 0.03 \times t^{1.933} + (A_m/V) \quad , (IPE) \quad (7)$$

Table 4 - Application limits for HEB and IPE cross sections regarding web component.

Standard fire resistance	Section factor (HEB)	Section factor (IPE)
R30	Am/V < 22.22	Am/V < 30.00
R60	Am/V < 15.38	Am/V < 18.56
R90	Am/V < 12.22	Am/V < 14.97
R120	Am/V < 11.11	-

The effect of the fire on the concrete was determined by the 500 °C isothermal (CEN, 2005). The external layer of concrete to be neglected may be calculated in both principal directions, defining $b_{c,fi,v}$ and $b_{c,fi,h}$. According to EN1994-1-2 (CEN, 2005), the thickness of concrete to

be neglected depends on section factor A_m/V , for standard fire resistance classes of R90 and R120. The new proposal (Paulo Piloto et al, 2015) demonstrates a strong dependence on the section factor for all standard fire resistance classes, see Eq. 8, and the applications conditions in Tables 5-6. The new proposal also differentiates the layer of concrete to be neglected in both principal directions. The average temperature of the residual concrete section may be calculated according to Eqs. 9-10. The new proposal introduces a parametric approximation, based on the standard fire resistance t and section factor A_m/V . The application limits are presented in Table 7. This calculation is affecting the second order moment of area of the concrete and also the elastic modulus of the material.

$$b_{c,fi} = a \times (A_m/V)^2 + b \times (A_m/V) + c \quad (8)$$

$$\theta_{c,t} = +3.1 \times t^{0.5} \times (A_m/V) + 0.003 \times t^{1.95} \quad , (HEB) \quad (9)$$

$$\theta_{c,t} = +2.67 \times t^{0.5} \times (A_m/V) + 3.4 \times t^{0.61} \quad , (IPE) \quad (10)$$

Table 5 - Parameters and application limits for thickness reduction of the concrete in sections HEB.

Standard fire resistance class	$b_{c,fi,h}$			$b_{c,fi,v}$			Section factor
	a	b	c	a	b	c	
R30	0,0000	0,0809	13,5	0,000	0,372	3,5	$10 \leq A_m/V \leq 25$
R60	0,1825	-4,2903	50,0	0,1624	-3,2923	41,0	$10 \leq A_m/V \leq 20$
R90	1,0052	-22,575	163,5	1,8649	-43,287	298,0	$10 \leq A_m/V \leq 17$
R120	0,0000	7,5529	-35,5	0,000	6,0049	9,0	$10 \leq A_m/V \leq 13$

Table 6 - Parameters and application limits for thickness reduction of the concrete in sections IPE.

Standard fire resistance class	$b_{c,fi,h}$			$b_{c,fi,v}$			Section factor
	a	b	c	a	b	c	
R30	0,0000	0,2206	10,5	0,0000	0,9383	-3,0	$14 \leq A_m/V \leq 30$
R60	0,2984	-8,8924	93,0	0,5888	-15,116	135,0	$14 \leq A_m/V \leq 22$
R90	1,3897	-38,972	313,0	2,0403	-50,693	393,0	$14 \leq A_m/V \leq 17$
R120	0,0000	18,283	-199,0	0,0000	48,59	-537,0	$14 \leq A_m/V \leq 15$

Table 7 - Application limits for average temperature of the concrete.

Standard fire resistance class	Section factor (HEB)	Section factor (IPE)
R30	$A_m/V < 25$	$A_m/V < 30$
R60	$A_m/V < 20$	$A_m/V < 23$
R90	$A_m/V < 17$	$A_m/V < 18$
R120	$A_m/V < 14$	$A_m/V < 15$

The effect of the fire into the reinforcement depends on the calculation of the average temperature of the material. The new parametric formula may be used to determine this effect. Eqs. 11-12 were developed, based on the distance between rebars and exposed surface u , fire resistance class t and section factor A_m/V . This calculation is affecting only the elastic modulus of the reinforcement.

$$\theta_{s,t} = 0.1 \times t^{1.1} \times (A_m/V) + 7.5 \times t - 0.1 \times t^{1.765} - 8 \times u + 390 \quad , (HEB) \quad (11)$$

$$\theta_{s,t} = 14.0 \times (A_m/V) + 11.0 \times t - 0.1 \times t^{1.795} - 8 \times u + 115 \quad , (IPE) \quad (12)$$

ADVANCED CALCULATION METHOD (FEM)

The nonlinear solution method was applied to calculate the temperature field. The finite element method requires the solution of Eq. 13 in the internal domain of the partially encased column and Eq. 14 in the external surface exposed to fire. In these equations: T represents the temperature of each material; $\rho(T)$ defines the specific mass; $C_p(T)$ defines the specific heat; $\lambda(T)$ defines the thermal conductivity; α_c specifies the convection coefficient; T_g represents the gas temperature of the fire compartment, using standard fire curve ISO 834 (ISO, 1999) around the cross section (4 exposed sides); Φ specifies the view factor; ε_m represents the emissivity of each material; ε_f specifies the emissivity of the fire; σ represents the Stefan-Boltzmann constant.

$$\nabla \cdot (\lambda_{(T)} \cdot \nabla T) = \rho_{(T)} \cdot C_{p(T)} \cdot \partial T / \partial t \quad (\Omega) \quad (13)$$

$$(\lambda_{(T)} \cdot \nabla T) \cdot \vec{n} = \alpha_c (T_g - T) + \Phi \cdot \varepsilon_m \varepsilon_f \cdot \sigma \cdot (T_g^4 - T^4) \quad (\partial\Omega) \quad (14)$$

The three-dimensional model uses element SOLID70 and LINK33 to model the profile / concrete and rebars, respectively. SOLID70 has a 3-D thermal conduction capability, presenting eight nodes with a single degree of freedom (temperature at each node). The interpolating functions are linear and uses full integration points (2x2x2) to define the conductivity matrix. The finite element LINK33 is a uniaxial element with the ability to conduct heat between two nodes. The element has a single degree of freedom, temperature at each node. The interpolating functions are linear and this element uses exact integration to define the conductivity matrix. Fig. 2 represents the shape of each element. Perfect contact between rebars and concrete is assumed, being the nodes of both elements shared in space. The nonlinear transient thermal analysis was defined with an integration time step of 60 s, which can decrease to 1 s and increase up to 120 s. The criterion for convergence uses a tolerance value of the heat flow, smaller than 0.1% with a minimum reference value of 1×10^{-6} .

The critical load was determined by an eigen buckling analysis, using the modification of finite elements. SOLID185 and SOLID65 were selected to model the steel profile and the concrete, while LINK180 was selected to model the rebars. SOLID185 is defined by eight nodes having three degrees of freedom at each node (translations in the nodal x, y, and z directions). This element has linear interpolating functions and can be used with different types of integration schemes. After a number of tests, reduced integration was selected. SOLID65 is also defined by eight nodes and the same degrees of freedom. This element was defined without internal rebars and with full integration (2x2x2). LINK180 was selected to model the rebars. This element has two nodes and a three degrees of freedom. The interpolating functions are linear and one point is used for integration.

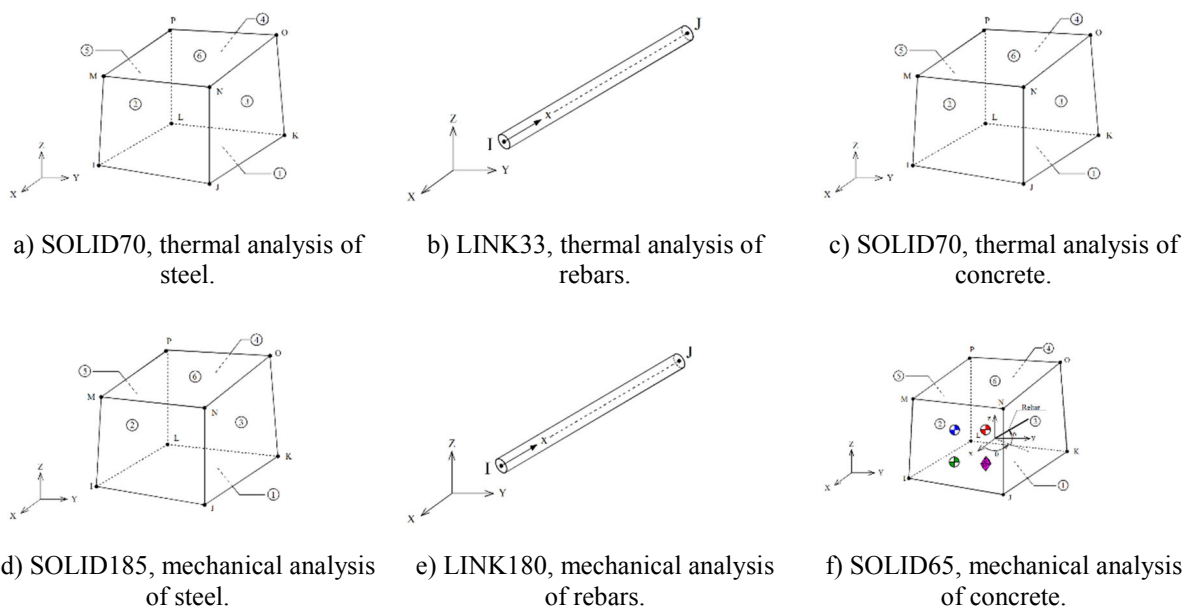


Fig. 2 - Finite elements used to build the three dimensional model of partially encased columns.

The temperature field was determined for the total time of 7200 s. Fig. 3 shows an example of the partially encased column exposed to ISO834 fire, after 30 and 60 minutes. The temperature field was recorded for the corresponding resistance class and applied as body load to the mechanical model. The mesh was defined after a solution convergence test.

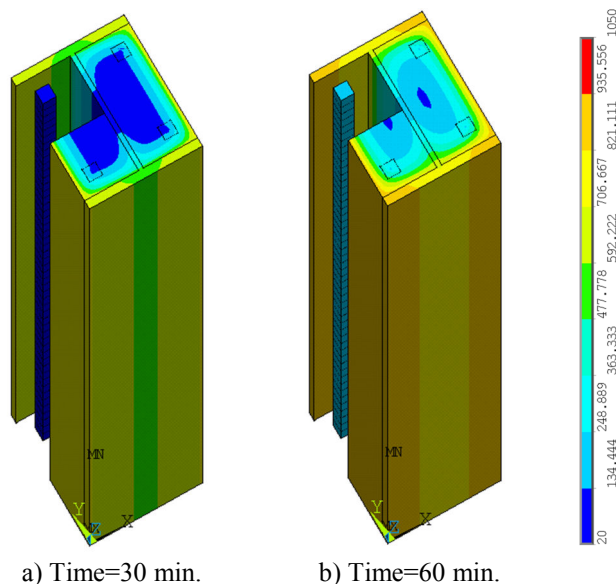


Fig. 3 - Numerical results for column HEB 360 and for different fire ratings classes.

The mechanical analysis uses static linear analysis as the basis for the buckling analysis. The solution of Eq. 15 must be find primarily, assuming $\{F_{ref}\}$ is an arbitrary load on the structure (usually a unit force). $[K]$ is its stiffness matrix and $\{d\}$ is the displacement vector. When the displacements are known, the stress field can be calculated for the reference load $\{F_{ref}\}$, which

can be used to form the stress stiffness matrix $[K_{\sigma,ref}]$. Since the stress stiffness matrix is proportional to the load vector $\{F_{ref}\}$, an arbitrary stress stiffness matrix $[K_{\sigma}]$ and an arbitrary load vector $\{F\}$ may be defined by a constant λ as shown by Eqs 16-17. The stiffness matrix is not changed by the applied load because the solution is linear. A relation between the stiffness matrices, the displacement and the critical load can then be presented as in Eq. 18, which can be used to predict the bifurcation point. The critical load is defined as $\{F_{cri}\}$. Since the buckling mode is defined as a change in displacement for the same load, Eqs. 18-19 are still valid, where $\{\delta d\}$ represents the incremental buckling displacement vector. The difference between Eq. 18 and Eq. 19 produces an eigenvalue problem, represented by Eq. 20 where the smallest root defines the first buckling load, when bifurcation is expected.

$$[K]\{d\} = \{F_{ref}\} \quad (15)$$

$$[K_{\sigma}] = \lambda[K_{\sigma,ref}] \quad (16)$$

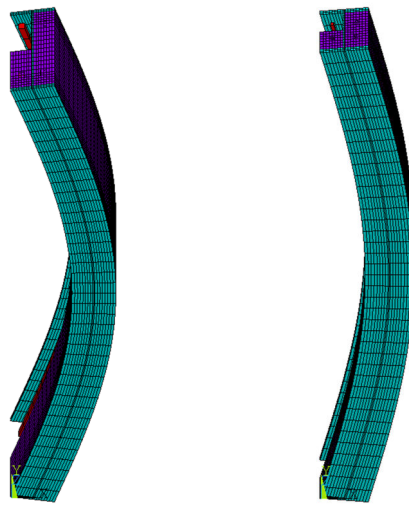
$$\{F\} = \lambda\{F_{ref}\} \quad (17)$$

$$[[K] + \lambda_{cri}[K_{\sigma,ref}]]\{d\} = \lambda_{cri}\{F_{ref}\} \quad (18)$$

$$[[K] + \lambda_{cri}[K_{\sigma,ref}]]\{\{d\} + \{\delta d\}\} = \lambda_{cri}\{F_{ref}\} \quad (19)$$

$$[[K] + \lambda[K_{\sigma,ref}]]\{\delta d\} = \{0\} \quad (20)$$

The trivial solution is not of interest, which means that the solution for λ is define for an algebraic equation, imposing the determinant of the global matrix equal to zero. The calculated eigenvalue is always related to an eigenvector $\{\delta d\}$ called a buckling mode shape, see Fig. 4. This numerical solution of a linear buckling analysis assumes that everything is perfect and therefore the real buckling load will be lower than the calculated buckling load if the imperfections are taking into account.



a) IPE330, after 30 min. b) HEB160 after 60 min.

Fig. 4 - Buckling results for different fire ratings classes.

RESULTS OF THE CRITICAL LOAD

The elastic buckling load is compared by two different solution methods. The simplified solution method applies to Eq. 4. The non-dimensional slenderness ratio may be calculated using Eq. 3, when the safety partial factors are equal to 1.0.

The advanced solution method applies to the results of the buckling analysis, using the finite element method.

Fig. 5 presents the comparison of the buckling load results, using the new proposal and the numerical solution, for 30 and 60 minutes of fire exposure.

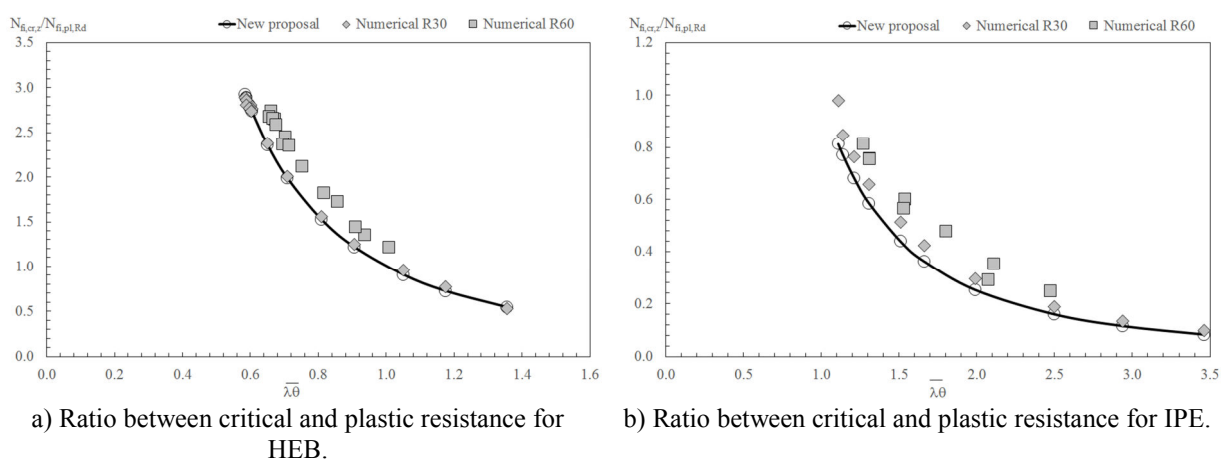


Fig. 5 - Comparison of the critical load between the new proposal and the numerical results.

CONCLUSION

Two different solution methods were applied to define the elastic buckling load of partially encased columns in case of fire. The new proposal is based on the balanced summation method proposed by EN 1994-1-2, but using safer formulas for the components to account for a reduction in geometry and an update of the material properties based on its average temperature.

The numerical solution method is based on the elastic buckling analysis, considering the resistance of the four components, taking into account the update of the material properties and the full geometry of column. This fact justifies that the numerical results are always higher than the ones presented by the new formulae.

This work is ongoing to compare the prediction of the buckling resistance of partially encased columns and to validate the best fitting curve for axial buckling load.

REFERENCES

- [1]-CEN - EN 1994-1-2; “Eurocode 4 - Design of composite steel and concrete structures-Part 1-2: General rules - Structural fire design”; Brussels, August 2005.
- [2]-Paulo Piloto, David Almeida, A. B Ramos-Gavilán, Luís M. R. Mesquita; “Partially Encased Section: Strength and Stiffness Under Fire Conditions”; pp: 15-18, Book of Abstracts of the IFireSS – International Fire Safety Symposium, ISBN 978-989-98435-3-0,

pp: 29-38, Book of full papers ISBN 978-989-98435-5-4, ISSN 2412-2629, University of Coimbra, Portugal, 20th-22nd April 2015.

[3]-ISO - ISO 834-1. Fire-resistance tests - Elements of building construction – Part 1: general requirements. Switzerland, Technical Committee ISO/TC 92: 25, 1999.

[4]-Cajot Louis-Guy, Gallois Louis, Debruyckere Rik, Franssen Jean-Marc, Simplified design method for slim floor beams exposed to fire, Proceedings of the Nordic Steel Construction Conference, Oslo, Norway, 5-7 September, 2012.

[5]-R. Zaharia, D. Duma, O.Vassart, Th. Gernay, J.M. Franssen, simplified method for temperature distribution in slim floor beams, Application of Structural Fire Design, Prague, Czech Republic, 29 April 2011.

[6]-R. Zaharia and J. M. Franssen, Simple equations for the calculation of the temperature within the cross-section of slim floor beams under ISO Fire, Steel and Composite Structures, Vol. 13, No. 2 (2012) pp 171-185. (doi: 10.12989/scs.2012.13.2.171).